Predicted thermophysical properties of UN, PuN, and (U,Pu)N

Galvin, Conor Oscar
Kuganathan, Navaratnarajah
Barron, Nicholas J
Grimes, Robin W

To be published in: Journal of Applied Physics

DOI to publisher's version: 10.1063/5.0177315

RESEARCH ARTICLE | APRIL 22 2024

Predicted thermophysical properties of UN, PuN, and (U,Pu)N

C. O. T. Galvin ; N. Kuganathan ; N. J. Barron ; R. W. Grimes

J. Appl. Phys. 135, 165101 (2024)
https://doi.org/10.1063/5.0177315

Journal of Applied Physics | ARTICLE | pubs.aip.org/aip/jap

Predicted thermophysical properties of UN, PuN, and (U,Pu)N

Cite as: J. Appl. Phys. **135**, 165101 (2024); doi: 10.1063/5.0177315
Submitted: 21 September 2023 · Accepted: 7 April 2024 ·
Published Online: 22 April 2024

View Online Export Citation CrossMark

C. O. T. Galvin,[1,2,a)] N. Kuganathan,[1] N. J. Barron,[3] and R. W. Grimes[2]

AFFILIATIONS

[1]Materials Science and Technology Division, Los Alamos National Laboratory, Los Alamos, New Mexico 87545, USA
[2]Department of Materials, Imperial College London, London SW7 2AZ, United Kingdom
[3]National Nuclear Laboratory Limited, Central Laboratory, Sellafield CA20 1PG, United Kingdom

[a)]**Author to whom correspondence should be addressed:** conor@lanl.gov

ABSTRACT

Molecular dynamics and density functional theory simulations are used to predict the lattice and electronic contributions of thermophysical properties for UN, PuN, and mixed (U,Pu)N systems. The properties predicted include the lattice parameter, linear thermal expansion, enthalpy, and specific heat capacity, as a function of temperature. The simulation predictions for high temperature specific heat capacity are compared against experimental measurements to understand the behavior, and why differences in the experimental measurements are observed. The influence of adding U vacancies, N interstitials, and Pu to UN is also examined. For this, a new PuN potential parameter set is developed and used with the Kocevski UN potential, enabling the dynamics of mixed (U,Pu)N systems to be studied. How defects impact the thermophysical properties is important for understanding fuel behavior under different reactor conditions, and these mechanistic predictions can be used to support fuel performance codes where data is scarce.

I. INTRODUCTION

Nitride nuclear fuels have been developed since the 1960s and were originally proposed as an alternative fuel form for fast neutron spectrum reactors.[1–3] Moreover, they have been investigated for use in space propulsion, and more recently, as one of the candidate fuels for several non-water cooled and advanced systems also known as Generation IV (Gen IV) reactors.[4,5] In addition, they are being investigated as accident tolerant and advanced technology fuels for next generation light water reactors (LWRs).[6–8] In comparison to conventional oxide fuels their higher thermal conductivity, higher fissile element density, and predicted good radiation tolerance make nitrides strong alternate fuel candidates. UN, for example, has a higher melting point than conventional oxide fuels; however, the melting point depends on nitrogen overpressurization.[9,10] Nitride fuels have already been tested successfully under operating fast reactor conditions.[11–14]

The beneficial properties of pristine UN compared to conventional oxide fuels could allow the fuel to operate at higher burn-ups, although it is unclear how defect formation alters properties. While there have been many experimental and theoretical studies on UN thermal properties,[15–19] there is still a lack of understanding in how defects affect thermal and mechanical properties; however, some studies have begun to address this.[20–22] Consequently, here atomic scale simulations are used to predict how specific defect configurations influence properties of UN.

Understanding the influence of defects is crucial if we are to predict how the fuel performs under reactor conditions. Simulations at the atomic scale contribute to our understanding by predicting the defect and temperature dependence of physical properties that dictate the mechanistic behavior that relates to macroscopic properties (though other macroscopic predictions are also important). Modern fuel performance codes employ knowledge of the physical processes that underpin property behavior to inform constituent parts of the performance codes. This approach can be particularly useful where limited data are available on which to base empirically fitted fuel behavior property models [which is the case for PuN and (U,Pu)N].

Both stoichiometry changes and formation of Pu species occur as a consequence of fuel burn-up. Thus, two classes of defect are considered: first, those associated with hyper-stoichiometry (both U vacancies and N interstitials) and second, the consequence of replacing U with Pu. In order to facilitate the latter, we predict the temperature dependent properties of PuN and then mixed stoichiometric (U,Pu)N systems.

Here, empirical potential based calculations are used to predict lattice parameter, linear thermal expansion coefficient (LTEC), change in enthalpy, and specific heat (at constant pressure) for UN and hyper-stoichiometric UN. We compare these predictions to available experimental data for UN, and address ambiguities between the high temperature experimental specific heat capacity measurements. Using the Kocevski *et al.*[22] UN potential N–N parameters, a new PuN potential was developed by fitting to the experimental PuN lattice parameter data. This provided the capability to predict thermophysical properties for PuN and mixed (U,Pu)N (10% and 20% additions of PuN to UN). Similar to the UN predictions, we were able to compare with available experimental data and make predictions where available data are limited. For the UN cases, more than one potential set is used to investigate properties where it is prudent to check how sensitive the results are to potential choice. As will be discussed later, having this comparison is important when interpreting the predictions of the specific heat capacity of UN and is important for choosing a UN potential to be used with the new developed PuN potential. For the electronic component of the specific heat capacity, electronic band structures were calculated using density functional theory (DFT) to solve the Boltzmann transport equation of both UN and PuN. DFT calculations are also used to examine the defect energies of UN, comparing to other DFT and molecular dynamics (MD) studies.

II. METHODOLOGY

A. Molecular dynamics simulations

1. Simulation approach

Equilibrium simulation predictions of thermophysical properties were carried out using the molecular dynamics (MD) Large-scale Atomic/Molecular Massively Parallel Simulator (LAMMPS) simulation package[23,24] under constant temperature and pressure (0 MPa) by applying an isothermal–isobaric (NPT) ensemble. Consequently, the system was able to undergo volume relaxation, without an external pressure. To achieve this, a Nosé–Hoover thermostat (with a damping value of 0.1 ps) and barostat (with a damping value of 0.5 ps) were used throughout.

2. Empirical potential sets

The potential set used to calculate the inter-atomic forces is a crucial factor in MD modeling as it controls the numerical and algorithmic simplicity and the fidelity of the simulations to reproduce the behavior of a material. Thus, it is important to know the applicability of the potential set to the objective of the simulations (i.e., is the simulation set selecting the right potential set for the property being investigated and does it reflect the physics that underlies that property?). A single type of atomic interaction modeled by one analytical function is not capable of reproducing all the different types of bonding in a material; therefore, different forms of inter-atomic potentials are normally tested. In this report, five potential parameter sets[20,22,25–27] found in the literature and describing the forces between the U and N atoms have been investigated.

MD simulation cells for defect-free UN and PuN were constructed by repeating the cubic rock salt unit cell 15 times in the three orthogonal directions, yielding a simulation box containing 27 000 atoms (i.e., a $15 \times 15 \times 15$ supercell). Hyper-stoichiometric UN simulation cells were generated in two ways: first, by randomly assigning N atoms to octahedral interstitial sites in the perfect supercell or second, by removing U atoms, until the desired defect concentration was reached. Similarly, mixed nitride systems were created by randomly assigning Pu atoms to U sites. In order to reduce the effect of bias introduced by any particular configuration, five distinct, random distributions were generated for each composition. Results shown later in this study were obtained by taking averages over these five configurations.

Following the creation of the structure, the system was equilibrated for 40 ps. This was used to minimize the effect of energy fluctuations in the system. This step is especially important for structures containing defects, in order to reduce the effect that local energetic configurations may have on further MD runs. MD calculations were then performed using a sequential temperature ramp with steps of 25 K from 300 to 2500 K for UN and with steps of 50 K from 300 to 2000 K for systems containing Pu. At each temperature, the system was equilibrated for 40 ps with the volume and enthalpy averaged over the final 4 ps. This allowed the system dimensions and enthalpy to be determined as a function of temperature.

3. Thermophysical properties

For the UN, PuN, and (U,Pu)N, the lattice parameter was predicted by taking the cube root of the systems volume. The linear thermal expansion coefficient is then derived similar to the study by Hayes *et al.*,[17]

$$\alpha = \frac{L - L_0}{L_0(T - T_0)}, \tag{1}$$

where L_0 is the lattice parameter at the reference temperature T_0, and L is the lattice parameter at temperature T. T_0 is taken as 300 K.

By plotting the enthalpy increment, H(T)–H(298 K), as a function of temperature (see Sec. II A C), the specific heat capacity, at a constant pressure can be determined from the first derivative of the enthalpy increment,

$$c_p = \frac{1}{n}\left(\frac{\partial H}{\partial T}\right)_p, \tag{2}$$

where n is the number of moles and $\frac{\partial H}{\partial T}$ is calculated by fitting a straight line to the enthalpy increment at a specific temperature and the points within 50 K on either side.

4. BoltzTrap2 calculations

The electronic contribution to the specific heat capacity was calculated by using the electronic band structure (calculated from quantum mechanical calculations described in Sec. II B below) to solve the semi-classical Boltzmann transport equation, under a relaxation time approximation implemented by the BoltzTrap2 code.[28]

B. Density functional theory

To capture electronic effects, density functional theory calculations were implemented using the Vienna *ab initio* Simulation Package (VASP).[29] This code solves standard Kohn–Sham equations using plane wave basis sets and projected augmented wave (PAW) pseudopotentials.[30] For all DFT calculations, a plane wave basis set with a cut-off of 500 eV and an $8 \times 8 \times 8$ Monkhorst–Pack[31] k-point mesh were used. An accurate representation of the materials properties requires a good approximation for many-body electron effects. This is captured by the exchange-correlation potential, and in this work the generalized gradient approximation (GGA) scheme defined by Perdew, Burke, and Ernzerhof (PBE)[32] was applied. However, the challenge in modeling U and Pu lies in their *f* electron behavior. Therefore, in order to describe the behavior of the localized *f* states, calculations were also conducted including the orbital dependent, Coulomb potential (Hubbard U), and the exchange parameter J, as formulated by Dudarev *et al.*[33] Using existing literature data,[34,35] values of $U = 2.50$ eV and $J = 0.125$ eV were applied to UN calculations, while values of $U = 3.20$ eV and $J = 0$ eV were applied for PuN calculations. The U values also consider the recommendation by Claisse *et al.*[36] that the value should be greater than 1.5 eV. For each relaxed configuration, the forces on the atoms were less than 0.001 eV/Å.

III. RESULTS AND DISCUSSION

In this section, for different UN systems, PuN and mixed (U,Pu)N, we predict the following: thermal dependence of lattice parameter, LTEC, enthalpy, and the specific heat at constant pressure.

Before the thermal dependent properties of UN were predicted, the literature MD potentials sets were tested for suitability. From the five potential sets examined,[20,22,25–27] two were rejected for further use after initial test simulations. These were the potential forms derived by Chen *et al.*[26] and Kurosaki *et al.*[25] With regard to Chen *et al.*,[26] it was found that the potential could not stabilize the UN structure for NPT calculations and it was rejected on this basis. Then, the Buckingham–Morse potential by Kurosaki *et al.*[25] was found to be unusable as key parameter set values were missing from the literature. In addition, the U, Pu, and N atoms of the Kurosaki *et al.*[25] potential sets contain charges. As the nitrides examined in this study behave like metallic systems, to capture the correct bonding behavior, they should have a charge of zero. The Kurosaki *et al.*[37] PuN potential set was, therefore, also rejected. The potential sets of Kuksin *et al.*[20] and Tseplyaev and Starikov[27] both delivered stable MD results, although they do not also have parameters to model PuN. Finally, the recent potential for UN, derived by Kocevski *et al.*,[22] was able to predict the thermophysical properties of UN. However, again there was no model for PuN. Therefore, a new PuN parameter set was developed, compatible with this UN potential as it uses the same N–N potential parameters, thereby giving the capability of predicting mixed (U,Pu)N properties (derivation of this potential was made possible through access to the same fitting procedure as used by Kocevski *et al.*[22]).

TABLE I. Parameters for the many-body interaction described by Eqs. (3)–(5). The arrow shows that the density of the atomic species on the left are being embedded in the other atomic species density, e.g., for N → Pu, the N atom density is being embedded in the density of the Pu atom.

	$F_{\alpha\beta}$ (eV Å^{-2})	$B_{\alpha\beta}$ (Å^{-2})	$r^0_{\alpha\beta}$ (Å)	n_α
N → Pu	3.0805	1.9481	1.3470	…
Pu → N	4.7887	1.2831	1.7459	…
N	…	…	…	0.5418
Pu	…	…	…	0.6287

A. New PuN potential

The PuN potential uses the same many-bodied Finnis–Sinclair EAM potential combined with a pairwise Buckingham term employed by Kocevski *et al.*

The potential energy, E_i, of an atom i with respect to all other atoms j is written as

$$E_i = F_\alpha\left(\sum_{j\neq i}\rho_{\alpha\beta}(r_{ij})\right) + \frac{1}{2}\sum_{j\neq i}\phi_{\alpha\beta}(r_{ij}),\ n_\alpha \neq 1, \tag{3}$$

where α and β represent the species of atoms i and j. The density function, $\rho_{\alpha\beta}(r_{ij})$), is specific to the type of interacting species. This differs from a "standard" EAM potential where the same density is used, no matter the species of the central atom. The term n^α ensures that the embedding function is non-linear.

The density function is described by

$$\rho_{\alpha\beta}(r_{ij}) = F_{\alpha\beta} r_{ij} \exp\left(-B_{\alpha\beta}\left(r_{ij} - r^0_{\alpha\beta}\right)^2\right),\ \alpha \neq \beta, \tag{4}$$

where $F_{\alpha\beta}$, $B_{\alpha\beta}$, and $r^0_{\alpha\beta}$ are empirical parameters dependent of the embedded atom and the density. $\phi_{\alpha\beta}(r_{ij})$ describes the pairwise interaction between atoms i and j. It has the Buckingham form where $A_{\alpha\beta}$ and $\rho_{\alpha\beta}$ are empirical parameters, shown in Eq. (5),

$$\phi_{\alpha\beta}(r_{ij}) = A_{\alpha\beta} \exp\left(-\frac{r_{ij}}{\rho_{\alpha\beta}}\right) - \frac{C_{\alpha\beta}}{r^6_{ij}}. \tag{5}$$

The C term is set to zero for this potential.

Parameters for the potential are outlined in Tables I and II. Due to a lack of single crystal elastic property experimental data for

TABLE II. Parameters for the Buckingham interaction described by Eq. (5).

$\alpha - \beta$	$A_{\alpha\beta}$ (eV)	$\rho_{\alpha\beta}$ (Å)
N–N	6611.7524	0.2338
Pu–Pu	1506.3201	0.3939
N–Pu	219.1329	0.4287

Journal of Applied Physics | ARTICLE | pubs.aip.org/aip/jap

TABLE III. Elastic constants (C_{xy}) and bulk modulus in GPa for the new PuN potential set compared to DFT values.[39] Note the predicted lattice parameter for this DFT work is 4.94 Å compared to 4.89 Å using the potential and 4.89 Å from experiment.

Property	MD (this work) (GPa)	DFT* (GPa)
C_{11}	311.5	280
C_{12}	112.4	92
C_{44}	57.1	63
Bulk modulus	178.8	154

PuN systems, this potential was fit only to the experimental lattice parameter data at different temperatures.[38] Elastic moduli for PuN predicted by this potential are reported in Table III and compare favorably to values derived using DFT.

B. Lattice parameter as a function of temperature

1. Uranium mononitride

Figure 1 shows the lattice parameters and LTEC as a function of temperature for UN and hyper-stoichiometric UN between 300 and 2500 K derived using the potentials of Kocevski *et al.*,[22] Kuksin *et al.*,[20] and Tseplyaev *et al.*[27] For U vacancy and N interstitial hyper-stoichiometric materials, the stoichiometry was $U_{0.98}N$ and $UN_{1.02}$, respectively. The black points are empirical correlations by Hayes *et al.*,[17] derived from collated experimental data sets. The red points are first principle predictions from Mei *et al.*[40] Although both the Kuksin and Tseplyaev potentials predict slightly lower lattice parameter values compared to experiment, the trend with temperature is similar. There is relatively good agreement with the experimental correlation given by Hayes *et al.*[17] and the Kocevski potential. However, while the lattice parameter as a function of temperature predicted using this potential is closer to the data by Hayes *et al.* than predicted by the previous potentials, the slope is slightly different. That is, the Kocevski potential slightly overestimates the lattice at lower temperatures and underestimates at higher temperatures, crossing through the experimental data at ∼1500 K.

At ambient temperature, all potential sets predict that the hyper-stoichiometric structure containing U vacancies exhibits a slightly lower lattice parameter compared to the perfect structure (because the uranium vacancy has a small negative defect volume). As temperature increases, the lattice parameter converges onto the

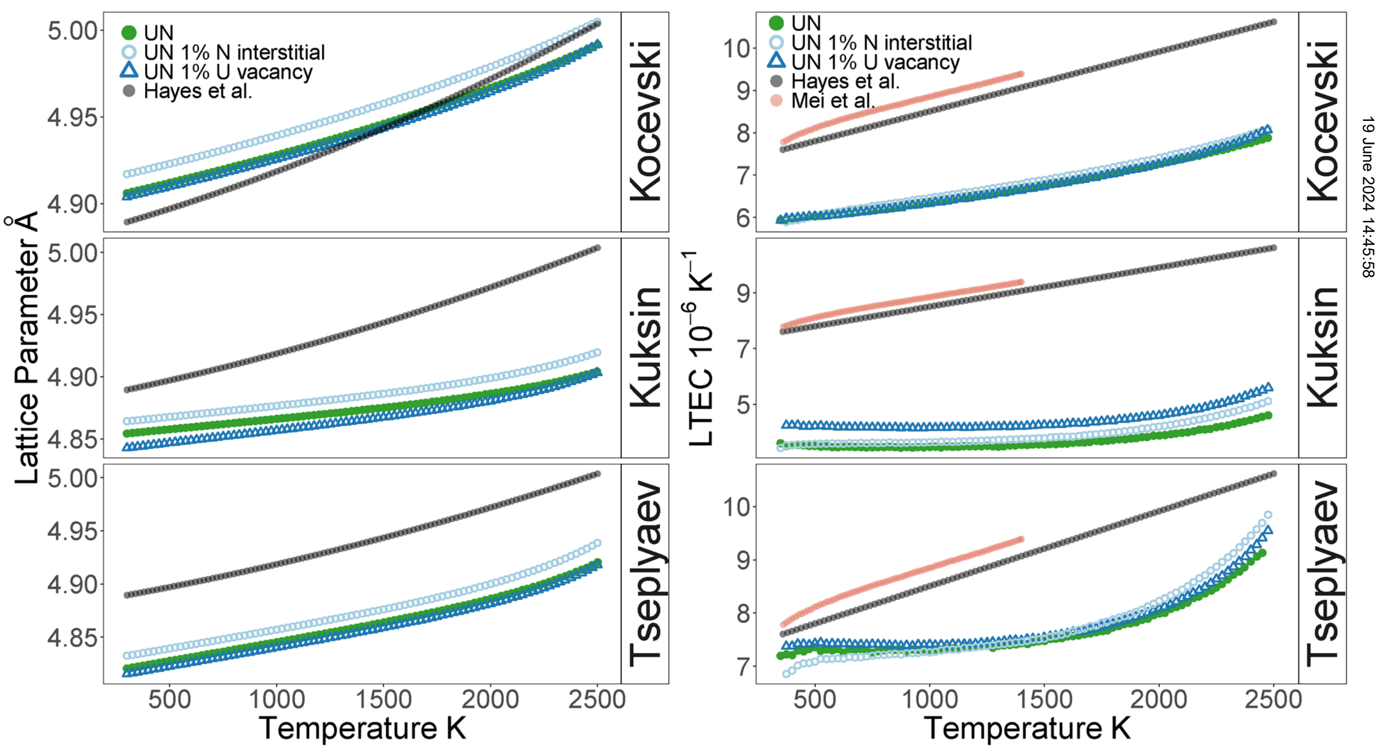

(a) (b)

FIG. 1. Predicted using MD based on the Kocevski, Kuksin, and Tseplyaev potentials: (a) the variation of lattice parameter as a function of temperature for UN, UN with U vacancies, and UN with N interstitials; (b) the linear thermal expansion coefficient as a function of temperature of UN, UN with U vacancies, and UN with N interstitials. A correlation of experimental results is given by the black points[17] and first principle calculations given by the red points.[40]

non-defective value. Conversely, with all potential sets, hyper-stoichiometric UN facilitated by N interstitials slightly raises the lattice parameter compared to the non-defective system, consistently over the temperature range (due to a small positive defect volume). Nevertheless, because the defect volumes are so small, the lattice parameter is not a strong function of U vacancy or N interstitial concentration. This is similar to what is seen for hypo-stoichiometric UN.[21] Furthermore, the LTEC values for stoichiometric and hyper-stoichiometric materials are practically identical over the whole temperature range, apart from that using the Kuksin potential, which shows a slight enhancement for U vacancies. This suggests that hyper-stoichiometry will not in itself give rise to lattice swelling or modify in how the lattice volume changes as a function of temperature. Nevertheless, other terms, for example, associated with the accumulation of fission products, may have an influence and these must eventually be considered.[41]

For the simulations presented in Figs. 1(a) and 1(b), the lattice parameter increases linearly with temperature until ∼1500 K, at which point the rate of growth increases non-linearly. This effect can be seen more clearly in the plots of linear thermal expansion coefficient, α, as a function of temperature [Fig. 1(b)]. Curiously, this change of rate for the lattice parameter with temperature is analogous to the superionic transition seen in UO_2, PuO_2, ThO_2, and MOx systems.[43–49] Underpinning this behavior in actinide oxides are defects generated in greater numbers at this temperature due to relatively low oxygen Frenkel energies, which are roughly ∼4−5 eV.[50] If the same were true in the case of UN, we would anticipate similarly low disorder reaction energies in UN. Therefore, the reaction energies for N Frenkel, U Frenkel, and Schottky disorder were predicted using each of the potentials (see Table IV). Similarly, these energies were calculated using the DFT approach described in Sec. II B, assuming 1 k anti-ferromagnetic order (see Table IV). It should be noted that different DFT methods can obtain different ground states for UN[34,51–55] And, therefore, influence the formation energies. In particular, the study by Kocevski *et al.*[42] outlines a detailed DFT study comparing different methods and takes an approach to address the metastable states that can arise using DFT+U by applying occupational matrix control. However, the trend of decreasing energy from Frenkel U to Frenkel N to Schottky is consistent across the DFT studies shown in Table IV. The formation energies given in Table IV indicate that the N Frenkel and Schottky pair reactions exhibit much lower formation energies than U Frenkel, but the N Frenkel and Schottky disorder energies are close. In fact, the potential due to Kocevski *et al.* and the current DFT simulations marginally favor the Schottky reactions, whereas previous DFT simulations and simulations using the potential due to Kuksin *et al.* or those due to Tseplysev *et al.* marginally favor the N Frenkel reaction over Schottky. It could then be that the creation of N Frenkel or Schottky defects contribute to the rapid growth in the linear thermal expansion coefficient above 1700 K—although as stated above, defect volumes are small so this is by no means definitive.

TABLE IV. Formation energies per defect (i.e., total reaction energy divided by two) in eV, predicted using the three potential sets used in this study, compared to DFT values.[20,42]

Defect	Kuksin (MD)	Tseplyaev (MD)	Kocevski (MD)	DFT (literature)	DFT (this work)
Frenkel U	7.87	8.94	14.36	7.1, 8.74	9.98
Frenkel N	4.04	4.47	4.01	4.9, 4.83	4.94
Schottky	4.43	4.52	3.90	4.96	3.36

2. Uranium and plutonium mononitride

The PuN potential was fit to the lattice parameter, resulting in the close agreement with experimental data[38] in Fig. 2. Adding UN to PuN lowers the lattice parameter and values lie between PuN and UN. Due to the Kocevski potential slightly overestimating the UN lattice parameter at low temperatures [Fig. 1(a)], it is expected that the lattice parameter for $(U_{90}, Pu_{10})N$ and $(U_{80}, Pu_{20})N$ is also slightly over-estimated (i.e., below 1000 K) as these mixed nitrides are heavily weighted toward UN. The predicted linear thermal expansion coefficients as a function of temperature for PuN and (U,Pu)N are shown in Fig. 3. Fits to the lattice parameter data are described by the following equation:

$$Lp(T) = \big(A_{UN}x + A_{PuN}(1-x)\big)T^2 + \big(B_{UN}x + B_{PuN}(1-x)\big)T + \big(C_{UN}x + C_{PuN}(1-x)\big), \quad (6)$$

where T is the temperature in K, and the fitted coefficients for A_{UN}, A_{PuN}, B_{UN}, B_{PuN}, C_{UN}, and C_{PuN} are reported in Table V while x describes the UN concentration (between 0 and 1). Electronic contributions are not expected to greatly impact the

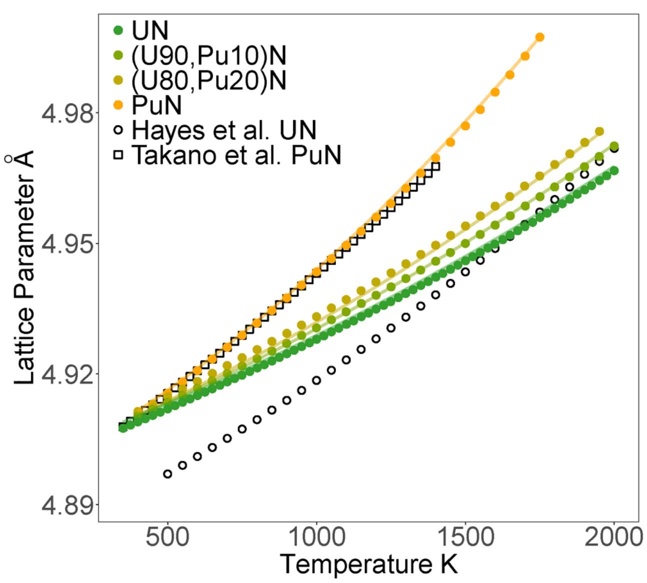

FIG. 2. The closed circles are MD calculated lattice parameter as a function of temperature for UN, PuN, and mixed (U,Pu)N. The open circles and squares represent experimental correlational and experimental values for UN and PuN, respectively. The lines are fits to the MD data described by Eq. (6).

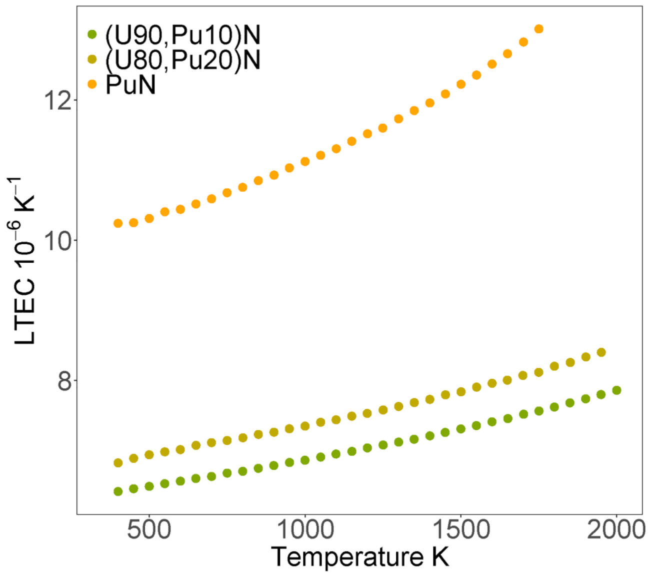

FIG. 3. Predicted LTEC for PuN and mixed (U,Pu)N.

TABLE V. Polynomial parameters for use with Eq. (6). All coefficients are in units Å.

$A_{UN}\times 10^{-9}$	$A_{PuN}\times 10^{-8}$	$B_{UN}\times 10^{-5}$	$B_{PuN}\times 10^{-5}$	C_{UN}	C_{PuN}
4.964	1.278	2.392	3.617	4.900	4.895

lattice parameter of UN or PuN, therefore these contributions are not included in the fit.

The model described by Eq. (6) provides a reasonable agreement with experimental lattice parameter values for (U,Pu)N across the temperature range 1500–2000 K (which extends beyond the operating temperature range for these mixed nitride fuels). For UN the potential predicts too low a slope across the full temperature range compared to the experimental data, slightly overestimating the lattice parameter at lower temperatures and underestimating at higher temperatures, but crossing through the experimental data at ∼1500 K. Therefore, it is not recommended to use this correlation with UN (or (U,Pu)N heavily weighted with UN) at temperatures much below 1500 K. That said, the UN potential is close to the experimental data between 1500 and 2000 K and with the PuN potential being fitted to experimental data, the fits

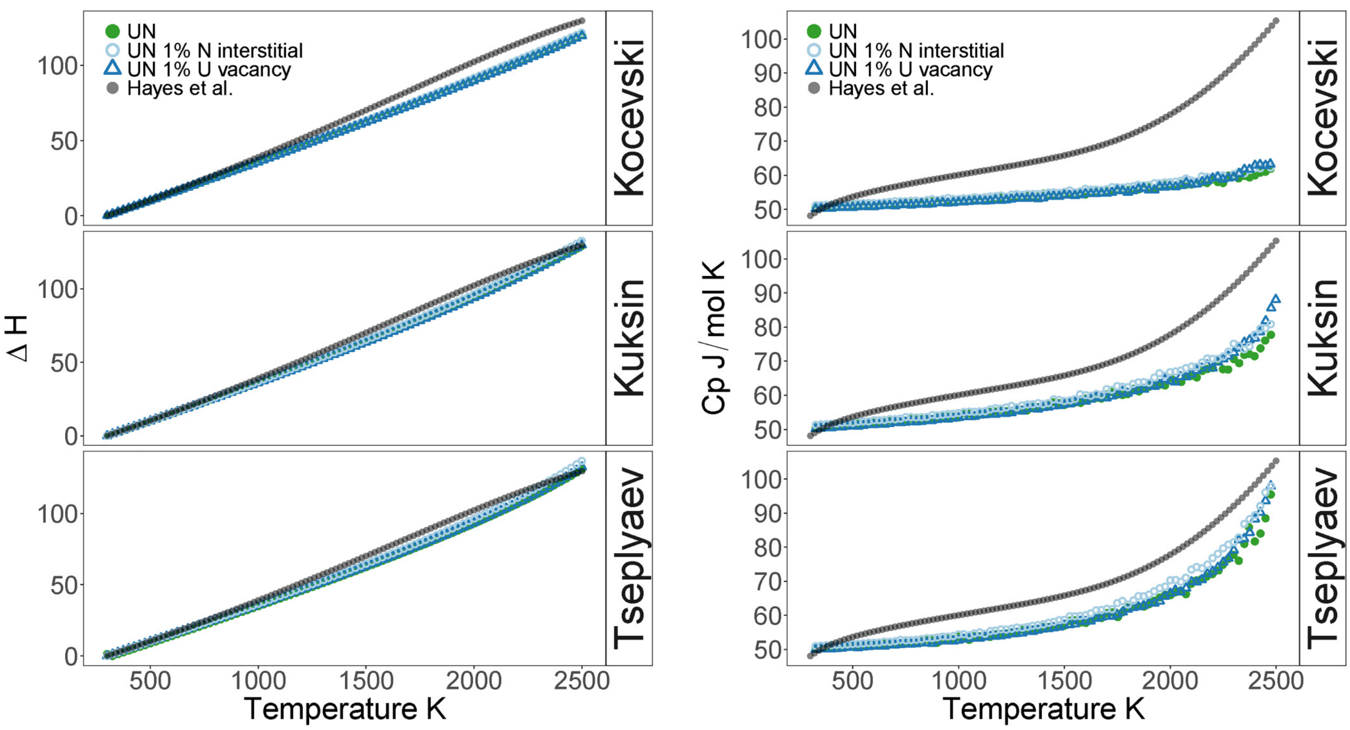

(a) (b)

FIG. 4. MD predictions of the lattice contributions to: (a) variation of enthalpy increment as a function of temperature for UN, UN with U vacancies, and UN with N interstitials. (b) The variation in specific heat capacity as a function of temperature. A correlation of experimental results is given by the black points.[18]

will give an accurate description of the thermal dependence of the lattice parameter for these systems over this temperature range. The mixed (U,Pu)N predictions from MD should then behave correctly across this temperature range and fitting to these (as well as UN and PuN) should yield a useful model between 1500 and 2000 K. An improved (U,Pu)N potential from 300 to 2000 K would be desirable to improve this model across this temperature range. Furthermore, there is a need for experimental values of mixed (U,Pu)N systems since data are scarce.

C. Enthalpy and specific heat

1. UN

The predicted changes in enthalpy [H(T)–H(298 K)] and specific heat calculated using constant pressure MD between 300 and 2500 K for UN and hyper-stoichiometric UN using the potentials of Kuksin *et al.* and Tslepeav *et al.* are presented in Fig. 4. In all cases, as the temperature increases, so does the enthalpy [Fig. 4(a)]. Thus, defects in the system associated with hyper-stoichiometry are not predicted to alter this behavior compared to the stoichiometric case.

As stated in the method section, Eq. (2), the specific heat capacities can be calculated from the derivative of the change in enthalpy and are presented in Fig. 4(b). Both the Kuksin and Tslepeav potentials predict a consistent growth in the specific heat until about 1500 K, at which point it increases more rapidly. This behavior is also a feature in the experimental data (this point is discussed further later in this section) and like the lattice parameter predictions, it is reminiscent of the superionic behavior in UO_2.

The potential of Kocevski *et al.* is also used to predict the MD enthalpy increment and specific heat of UN (see Fig. 4). As with the other two potential sets, the enthalpy increment is predicted to gradually increase in value leading to a growth in specific heat value. However, unlike the previous results, a more rapid increase does not begin until well over 2000 K, and even then it is much more modest even though the defect formation energies are similar for all three potentials (Table IV).

The simulations illustrated in Fig. 4 only capture the lattice contribution to specific heat and not the contribution of 5*f* electron excitations that could also account for the increase in specific heat (which is known to be the case over low temperature ranges, that is, 300–900 K, in uranium systems[56,57]). Figure 5 shows the specific heat capacity predicted using the three potentials via MD (i.e., only the lattice contribution) but also, MD results corrected for the electronic contributions, calculated by solving Boltzmann transport equations (described in Sec. II A 4). Electronic contributions to the specific heat capacity of UN and PuN were calculated by solving Boltzmann transport equations (see Sec. II A 4) and are presented in Fig. 6. By comparing with values in Fig. 4, it is clear that electronic contributions are only slightly smaller than the lattice contributions, which is consistent with other studies.[40,58] Figure 5 also shows the correlation data of Hayes *et al.*, predictions using density functional perturbation theory (DFPT) by Mei *et al.*,[40] and the two available high temperature experimental datasets by Affortit,[59] and Conway and Flagella[60] (discussed below).

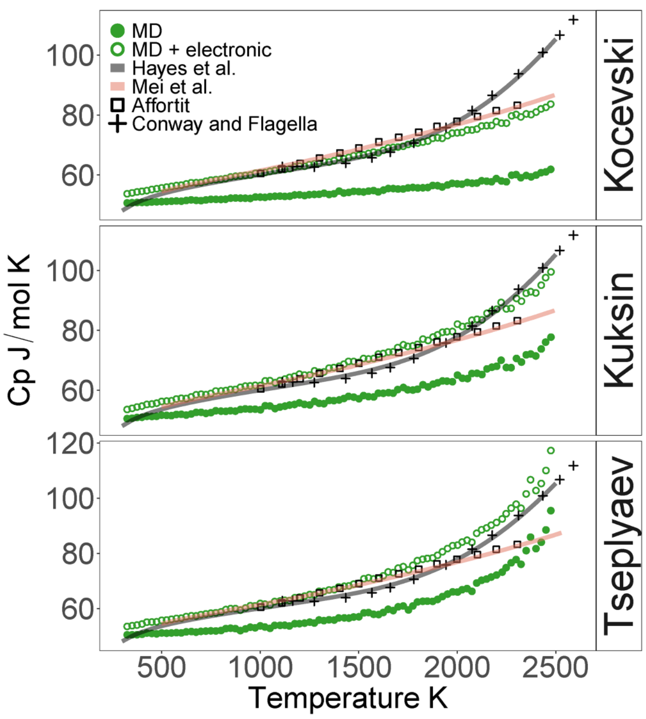

FIG. 5. The specific heat capacity as a function of temperature for three MD potential sets, with and without electronic correction, compared to experimental data[18,59,60] and a DFPT study by Mei *et al.*[40]

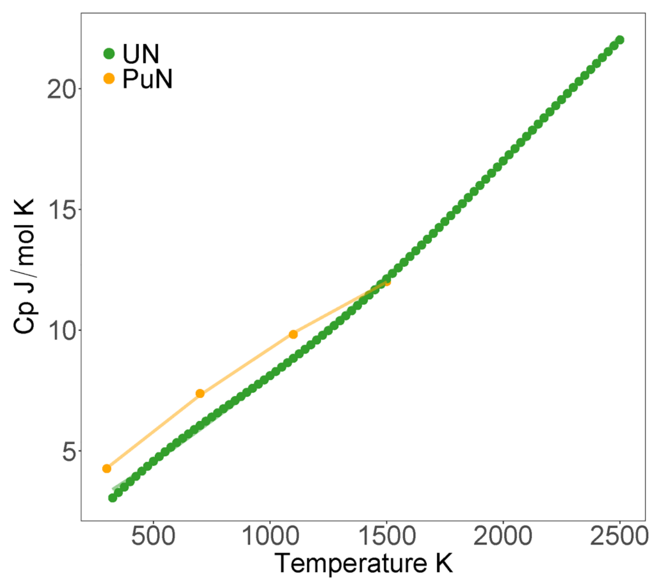

FIG. 6. Electric contributions to the specific heat capacity for UN and PuN as a function of temperature. The fits given by Eq. (7) are shown as lines.

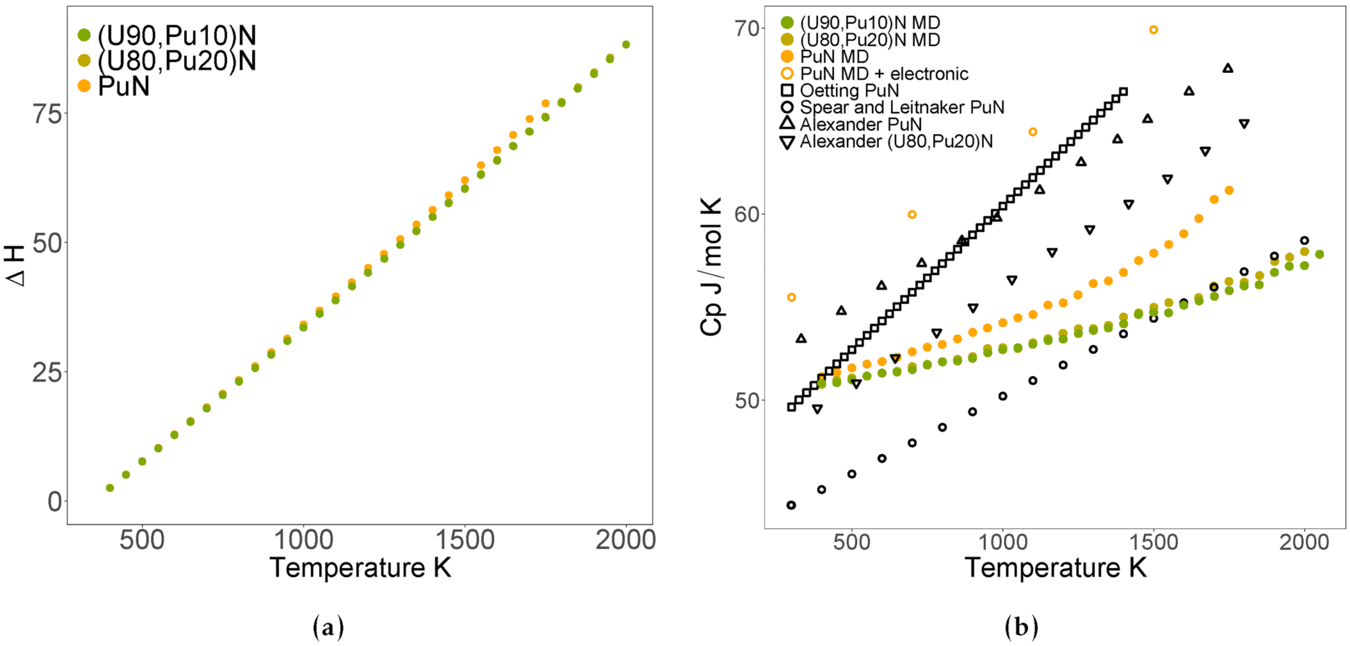

FIG. 7. The variation of enthalpy increment as a function of temperature for PuN, (U_{90}, Pu_{10})N, and (U_{80}, Pu_{20})N is shown in (a), and (b) depicts the variation in specific heat capacity as a function of temperature. The summed lattice and electronic contributions for PuN are represented by circles.

Considering the total specific heat capacity (electronic and lattice contributions, Fig. 5), it is observed that two of the potentials (Kuksin and Tseplyaev) predict a rapid rise and are in good agreement with the Conway and Flagella data (see Fig. 5). These potentials were not fitted to specific heat or enthalpy data but still predict this behavior. The Kocevski potential[22] does not predict this rapid rise but has a trend similar to the data of Affortit[59] and the modeling predictions using DFPT by Mei *et al.*[40]

Many studies have been carried out to calculate the specific heat of UN as a function of temperature using calorimeter and laser flash experimental techniques as well as thermodynamic relationships.[9] It was from eight different such datasets that the correlation equation developed by Hayes *et al.* was derived. In general, most of the experimental work is in good agreement, and, thus, a good understanding of the behavior can be assumed. However, there are some discrepancies at higher temperatures. Between 1000 and 1700 K, most of the data appear consistent apart from measurements by Affortit,[59] where both the magnitude and the slope differ from other available experimental data. This disagreement could be a result of the experimental technique employed by Affortit, which involved the rapid heating of a UN wire. Therefore, the data by Affortit were not used as one of the datasets by Hayes *et al.* when developing their correlation model.

Above 1700 K, there are only two sets of experimental data: those of Affortit[59] and Conway and Flagella.[60] The work by

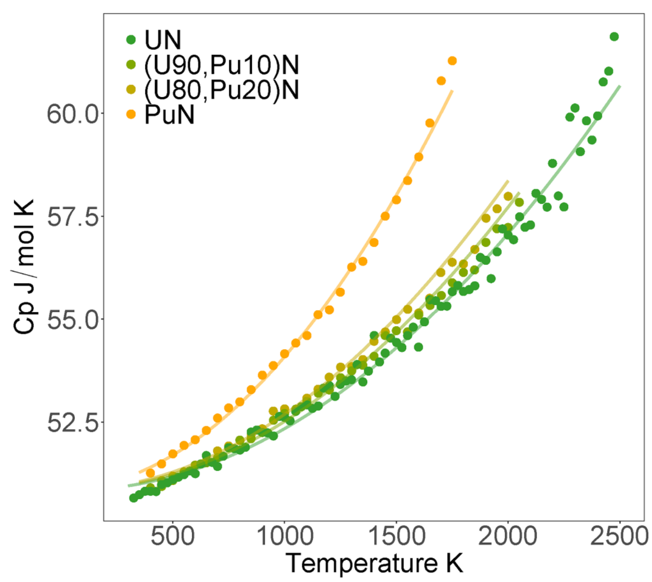

FIG. 8. MD calculated lattice contributions to the specific heat capacity for UN, PuN, and mixed (U,Pu)N as a function of temperature. The fits given by Eq. (7) are shown as lines.

TABLE VI. Polynomial parameters for use with Eq. (7) for the phonon contribution to the specific heat capacity. All coefficients are in units J/mol K.

$A_{UN} \times 10^{-9}$	$A_{PuN} \times 10^{-9}$	$B_{UN} \times 10^{-7}$	$B_{PuN} \times 10^{-7}$	$C_{UN} \times 10^{-2}$	$C_{PuN} \times 10^{-2}$
1.621	3.072	−1.210	1.743	5.084	5.084

Conway and Flagella shows a rapid upward increase of specific heat values above ∼1700 K. Their work consists of enthalpy measurements, used to calculate the specific heat, performed on samples containing 79.7 wt. % UN and 20.3 wt. % UO_2.[18,60] The enthalpy was assumed to be the sum of the products of enthalpy and the weight fractions of UN and UO_2. The enthalpy of UO_2 is well understood and above 1700 K, a superionic transition is known to occur which would be evident in the results. A similar rapid upward rise in specific heat capacity is seen at high temperatures in other actinide fuels, such as oxides and carbides and is the result of the formation of defects.[9,61] However, as highlighted above, there is a paucity of equivalent data for UN above 1700 K and, furthermore, UN is known to dissociate at these temperatures.[9,18,62] The heat capacity correlated equation of Hayes *et al.* includes the results of Conway and Flagella. These data were also chosen as it is in good agreement with available data over the temperature range 1000–1700 K. However, the work of Affortit was not included.

It is clear that further work is required, both simulation and experiment to understand to what extent there is actually a rapid increase in specific heat of UN at higher temperatures and to identify its origin. The simulation data may suggest that a defect production mechanism is not being captured by the Kocevski potential (see defect energies in Table IV), but that is far from clear. If a defect mechanism is not the cause of the rise in specific heat capacity, another process must be operating such as softening of a phonon mode or more generally an increase in the magnitude of lattice vibrations (greater anharmonicity). Specific heat is effectively a measure of how much heat is locked up as potential energy in the system. This can happen as atoms vibrate about their sites. As they vibrate further from their lattice points, in terms of classical MD simulations, the atoms move further up the potential energy well binding them to their sites—meaning more heat needs to be pumped into the system as the temperature increases. It is also possible that the Kocevski potential captures the correct behavior and this rapid rise observed by Conway and Flagella (and the other two potential sets) is not a true representation of the specific heat capacity behavior at high temperatures (i.e., above 1700 K). As such, this experimentally observed rapid rise could be a consequence of another process such as dissociation of the UN. With so many uncertainties and the lack of existing experimental data, new high temperature measurements (above 1700 K) of specific heat of UN would be valuable.

2. (U,Pu)N

The predicted enthalpy increment [H(T)–H(298 K)] for PuN increases with temperature, as shown in Fig. 7(a), and as with UN, this is used to calculate the specific heat capacity [see Fig. 7(b)]. Specific heat capacity information for PuN is scarce and the three experimental datasets presented in Fig. 7(b) differ greatly. It has been argued that the data by Oetting[63] is more reliable and is usually recommended.[9] However, the trend for the total specific heat-temperature curves (electronic and lattice), shown by blue points in Fig. 7(b), predicted here agrees better with the values calculated by Alexander[9,64] overall, and in particular, the temperature dependence is close. That said, the values at high temperatures (above 1500 K) are closer to those by Oetting.[63] The PuN specific heat values by Spear and Leitnaker[65] are much lower than all other values (predicted and experiment).

The lattice contributions to specific heat are also predicted for two compositions of mixed nitrides [$(U_{90}, Pu_{10})N$ and $(U_{80}, Pu_{20})N$] [see Fig. 7(b)]. These are lower than the lattice contribution to the specific heat for PuN. This reduction is consistent with the experimental work by Alexander.[64] However, the reduction is not consistently smaller over the temperature range. These values are close to the values of PuN at low temperatures and do not rise as quickly as temperature increases. This could be due to the UN part predicted by the Kocevski potential not rising as rapidly, as discussed in Sec. III B 2. There is little difference between the specific heat values of $(U_{90}, Pu_{10})N$ and $(U_{80}, Pu_{20})N$.

A quadratic equation fitted to atomistic data describes the specific heat capacity as a function of temperature (300–2000 K) for (U,Pu)N. The specific heat is presented as its lattice and electrical contributions, respectively. Phonon contributions to the specific heat capacity of UN, $(U_{90}, Pu_{10})N$, $(U_{80}, Pu_{20})N$, and PuN were calculated from the changes in enthalpy [H(T)–H(298 K)] predicted by MD simulations and are presented in Fig. 8. The lines in Fig. 8 represent fits to the data given by

$$Cp_{phonon}(T) = \big(A_{UN}x + A_{PuN}(1-x)\big)T^2 + \big(B_{UN}x + B_{PuN}(1-x)\big)T + \big(C_{UN}x + C_{PuN}(1-x)\big), \tag{7}$$

where T is temperature in K, and A_{UN}, A_{PuN}, B_{UN}, B_{PuN}, C_{UN}, and C_{PuN} are fitting coefficients while x describes the UN concentration

TABLE VII. Polynomial parameters for use with Eq. (7) for the electronic contribution to the specific heat capacity. All coefficients are in units J/mol K.

$A_{UN} \times 10^{-9}$	$A_{PuN} \times 10^{-9}$	$B_{UN} \times 10^{-6}$	$B_{PuN} \times 10^{-6}$	$C_{UN} \times 10^{-3}$	$C_{PuN} \times 10^{-3}$
1.126	−1.435	5.450	9.002	1.518	1.716

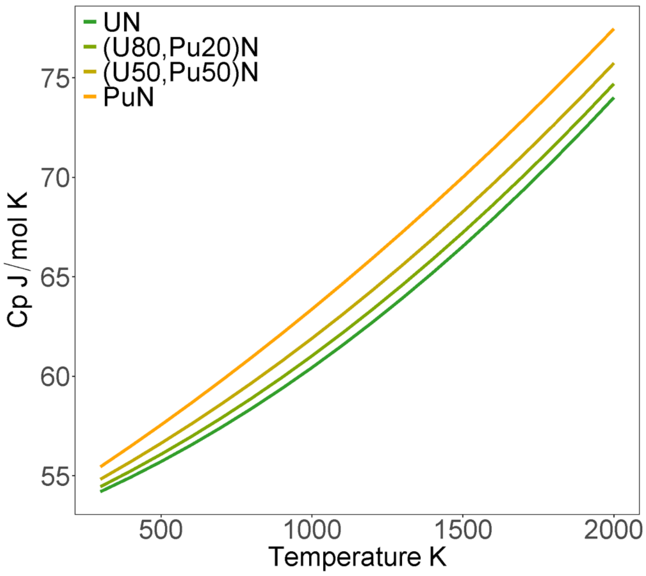

FIG. 9. Lines predicting the total specific heat capacity of UN, $(U_{90}, Pu_{10})N$, $(U_{50}, Pu_{50})N$, and PuN from the summation of the electronic and lattice contributions.

dependence (between 0 and 1). Table VI reports the fitting parameter values for Eq. (7).

As presented in Sec. III B 4, the electronic contributions to the specific heat capacity of UN and PuN were calculated by solving Boltzmann transport equations. A linear interpolation between UN and PuN was assumed for the mixed (U,Pu)N nitride systems. A fit applied to these results based on the same analytical form as Eq. (7) gives rise to the coefficients reported in Table VII.

The total specific heat capacity for UN, PuN, and mixed (U,Pu)N is shown in Fig. 9, derived by summing the phonon and electronic contributions. Interestingly, for the intermediate composition, once the electronic terms are included, value sit more centrally between UN and PuN than do values predicted just on lattice contributions (compare Figs. 8 and 9).

IV. CONCLUSIONS

This study employed atomistic simulation techniques to investigate the temperature dependent thermophysical properties of UN and hyper-stoichiometric UN. Three different sets of UN interatomic potentials were used to calculate lattice contributions to properties and DFT based simulations to calculate electronic contributions. A new PuN potential parameter set was developed, consistent with the Kocevski UN potential, allowing PuN and mixed (U,Pu)N systems to be studied here. The simulation predictions can be implemented in fuel performance codes, which rely on information such as thermophysical properties, to predict accurate fuel pin behavior. Furthermore, this potential will enable future MD simulations to be conducted advancing the understanding of (U,Pu)N, where data are scarce.

For UN, it was found that all the properties predicted compared well with experiment. Modest additions of N interstitials or U vacancies, corresponding to hyper-stoichiometry, had little or negligible impact on predicted property values. Again, this information is important as defects like these will occur in UN fuel under reactor conditions. As expected, for all UN properties investigated, the electronic contribution had the greatest impact on the specific heat capacity as a function of temperature. For the lattice contribution to the specific heat capacity, the three potential sets all predicted similar behavior up to ∼1700 K. However, above 1700 K, different behavior was observed with two potentials predicting a rapid rise of specific heat at high temperatures, while one does not. For the high temperature predictions, there are only two experimental datasets for the specific heat capacity of UN with which to compare. There is a clear discrepancy between these two experimental datasets and for both studies, there are still questions about the reliability of the results. Using our predictions, we discuss possible underlying causes for this discrepancy and suggest that new high temperature measurements of the specific heat capacity of UN are required.

For PuN and (U,Pu)N, the new potential predicts values close to available experimental results; however, experimental data are scarce. As the UN Kocevski potential slightly overestimates the lattice parameter for lower temperatures and underestimates for higher temperatures, crossing through the experimental data at ∼1500 K, it is highly likely that (U,Pu)N heavily weighted with UN would do the same. That said, the UN potential is close to the experimental data between 1500 and 2000 K and with the PuN potential being fitted to experimental lattice parameter data, an accurate description of the lattice parameter for (U,Pu)N should apply across this temperature range.

There are a handful of experimental results to compare the predicted specific heat capacity of PuN, but the experimental results vary widely. The simulation predictions help in understanding the experimental measurements, but, like UN, new experiments for high temperature specific heat capacity of PuN and (U,Pu)N would also be valuable. Due to the scarcity of reliable experimental values above 1500 K but good agreement with specific heat experiments below this temperature, it is probable that the atomic scale predictions will yield reliable results for (U,Pu)N (with high percentage of UN) only up to 1500 K.

SUPPLEMENTARY MATERIAL

The supplementary material provides the tabulated (U,Pu)N potential file used for this work.

ACKNOWLEDGMENTS

This research was funded under the £46m Advanced Fuel Cycle Programme as part of the Department for Business, Energy and Industrial Strategy's (BEIS) £505m Energy Innovation Programme. We acknowledge support of the authors of Kocevski *et al.*[22] in deriving the PuN potential.

AUTHOR DECLARATIONS

Conflict of Interest

The authors have no conflicts to disclose.

Author Contributions

C. O. T. Galvin: Conceptualization (supporting); Data curation (lead); Formal analysis (lead); Investigation (lead); Project administration (supporting); Writing – original draft (equal); Writing – review & editing (equal). **N. Kuganathan:** Data curation (supporting); Investigation (supporting); Writing – original draft (supporting). **N. Barron:** Conceptualization (supporting); Funding acquisition (equal); Investigation (supporting); Project administration (equal); Writing – review & editing (supporting). **R. W. Grimes:** Conceptualization (equal); Formal analysis (supporting); Funding acquisition (equal); Investigation (supporting); Project administration (equal); Supervision (equal); Writing – original draft (equal); Writing – review & editing (equal).

DATA AVAILABILITY

The data that support the findings of this study are available from the corresponding author upon reasonable request.

REFERENCES

[1]W. M. Pardue, V. W. Storhok, R. A. Smith, and D. L. Keller, "An evaluation of plutonium compounds as nuclear fuels," Nucl. Met., Met. Soc. AIME **13**, 369–381 (1964).
[2]J. M. Cleveland, G. H. Bryan, C. R. Heiple, and R. J. Sironen, "A new, low-temperature synthesis of plutonium and uranium nitrides," Nucl. Technol. **25**(3), 541–545 (1975).
[3]C. T. Walker, "Investigation of irradiated uranium-plutonium carbonitride fuel by microprobe analysis," Nucl. Technol. **39**(3), 289–296 (1978).
[4]R. B. Matthews, K. M. Chidester, C. W. Hoth, R. E. Mason, and R. L. Petty, "Fabrication and testing of uranium nitride fuel for space power reactors," J. Nucl. Mater. **151**(3), 345 (1988).
[5]Y. Arai, "Nitride fuel," in *Comprehensive Nuclear Materials* (Elsevier, 2012), pp. 41–54.
[6]C. Ekberg, D. R. Costa, M. Hedberg, and M. Jolkkonen, "Nitride fuel for Gen IV nuclear power systems," J. Radioanal. Nucl. Chem. **318**(3), 1713–1725 (2018).
[7]K. D. Johnson and D. Lopes, "Grain growth in uranium nitride prepared by spark plasma sintering," J. Nucl. Mater. **503**, 75–80 (2018).
[8]K. Yang, E. Kardoulaki, D. Zhao, A. Broussard, K. Metzger, J. T. White, M. R. Sivack, K. J. Mcclellan, E. J. Lahoda, and J. Lian, "Uranium nitride (UN) pellets with controllable microstructure and phase—Fabrication by spark plasma sintering and their thermal-mechanical and oxidation properties," J. Nucl. Mater. **557**, 153272 (2021).
[9]M. Uno, T. Nishi, and M. Takano, "Thermodynamic and thermophysical properties of the actinide nitrides," in *Comprehensive Nuclear Materials* (Elsevier, 2012), pp. 61–85.
[10]U. Carvajal Nunez, D. Prieur, R. Bohler, and D. Manara, "Melting point determination of uranium nitride and uranium plutonium nitride: A laser heating study," J. Nucl. Mater. **449**(1-3), 1–8 (2014).
[11]V. V. Orlov, V. S. Smirnov, V. S. Skikunov, A. I. Filin, V. V. Naumov, S. V. Bulavkin, B. D. Rogoskin, M. G. Shishkov, O. N. Dubrovin, N. M. Stepennova, and Y. E. Fedorov, "Mononitride fuel and large scale nuclear power industry," in *Moscow All Russian Scientific and Research Institute of Inorganic Materials* (OSTI, 1997).
[12]R. Bruce Matthews, "Irradiation performance of nitride fuels," No. LA-UR-93-2392; CONF-9309172-1. Los Alamos National Lab., New Mexico, 1993.
[13]S. B. Ross, M. S. El-Genk, and R. B. Matthews, "Uranium nitride fuel swelling correlation," J. Nucl. Mater. **170**(2), 169–177 (1990).
[14]F. N. Kryukov, O. N. Nikitin, S. V. Kuzmin, A. V. Belyaeva, E. B. Maltseva, I. F. Gilmutdinov, and P. I. Grin, "State of nitride fuel after irradiation in fast reactors," Atomic Energy **112**(6), 410–416 (2012).
[15]K. Kurosaki, K. Yano, K. Yamada, M. Uno, and S. Yamanaka, "A molecular dynamics study of the heat capacity of uranium mononitride," J. Alloys Compd. **297**(1–2), 1–4 (2000).
[16]K. Kurosaki, K. Yano, K. Yamada, M. Uno, and S. Yamanaka, "A molecular dynamics study of the thermal conductivity of uranium mononitride," J. Alloys Compd. **311**(2), 305–310 (2000).
[17]S. L. Hayes, J. K. Thomas, and K. L. Peddicord, "Material property correlations for uranium mononitride. I. Physical properties," J. Nucl. Mater. **171**(2–3), 262–270 (1990).
[18]S. L. Hayes, J. K. Thomas, and K. L. Peddicord, "Material property correlations for uranium mononitride," J. Nucl. Mater. **171**(2–3), 300–318 (1990).
[19]V. Kocevski, D. A. Rehn, A. J. Terricabras, A. van Veelen, M. W. D. Cooper, S. W. Paisner, S. C. Vogel, J. T. White, and D. A. Andersson, "Finite temperature properties of uranium mononitride," J. Nucl. Mater. **576**, 154241 (2023).
[20]A. Yu. Kuksin, S. V. Starikov, D. E. Smirnova, and V. I. Tseplyaev, "The diffusion of point defects in uranium mononitride: Combination of DFT and atomistic simulation with novel potential," J. Alloys Compd. **658**, 385–394 (2016).
[21]J. J. Li and S. T. Murphy, "Diffusion in hypo-stoichiometric uranium mononitride," Prog. Nucl. Energy **142**(10), 103995 (2021).
[22]V. Kocevski, M. W. D. Cooper, A. J. Claisse, and D. A. Andersson, "Development and application of a uranium mononitride (UN) potential: Thermomechanical properties and Xe diffusion," J. Nucl. Mater. **562**, 153553 (2022).
[23]S. Plimpton, "Fast parallel algorithms for short-range molecular dynamics," J. Computational Phys., **117**(1), 1–19 (1995).
[24]A. P. Thompson, H. M. Aktulga, R. Berger, D. S. Bolintineanu, W. M. Brown, P. S. Crozier, P. J. in 't Veld, A. Kohlmeyer, S. G. Moore, T. D. Nguyen, R. Shan, M. J. Stevens, J. Tranchida, C. Trott, and S. J. Plimpton, "LAMMPS—A flexible simulation tool for particle-based materials modeling at the atomic, meso, and continuum scales," Comput. Phys. Commun. **271**, 108171 (2022).
[25]K. Kurosaki, K. Yano, K. Yamada, M. Uno, and S. Yamanaka, "A molecular dynamics study on uranium–plutonium mixed nitride," J. Alloys Compd. **319**(1–2), 253–257 (2001).
[26]P. H. Chen, X. L. Wang, X. C. Lai, G. Li, B. Y. Ao, and Y. Long, "Ab initio interionic potentials for UN by multiple lattice inversion," J. Nucl. Mater. **404**(1), 6–8 (2010).
[27]V. I. Tseplyaev and S. V. Starikov, "The atomistic simulation of pressure-induced phase transition in uranium mononitride," J. Nucl. Mater. **480**, 7–14 (2016).
[28]G. K. H. Madsen, J. Carrete, and M. J. Verstraete, "BoltzTraP2, a program for interpolating band structures and calculating semi-classical transport coefficients," Comput. Phys. Commun. **231**, 140–145 (2018).
[29]G. Kresse and J. Furthmüller, "Efficient iterative schemes for ab initio total-energy calculations using a plane-wave basis set," Phys. Rev. B **54**(16), 11169–11186 (1996).
[30]P. E. Blöchl, "Projector augmented-wave method," Phys. Rev. B **50**(24), 17953–17979 (1994).
[31]H. J. Monkhorst and J. D. Pack, "Special points for Brillouin-zone integrations," Phys. Rev. B **13**(12), 5188–5192 (1976).
[32]J. P. Perdew, K. Burke, and M. Ernzerhof, "Generalized gradient approximation made simple," Phys. Rev. Lett. **77**(18), 3865–3868 (1996).
[33]S. L. Dudarev, G. A. Botton, S. Y. Savrasov, C. J. Humphreys, and A. P. Sutton, "Electron-energy-loss spectra and the structural stability of nickel oxide: An LSDA+U study," Phys. Rev. B **57**(3), 1505–1509 (1998).
[34]D. Gryaznov, E. Heifets, and E. Kotomin, "The first-principles treatment of the electron-correlation and spin–orbital effects in uranium mononitride nuclear fuels," Phys. Chem. Chem. Phys. **14**(13), 4482 (2012).
[35]C. Lai, Y. Hu, and R. Qiu, "Exploring the sub-stoichiometric behavior of plutonium mononitride," RSC Adv. **10**, 24877–24881 (2020).
[36]A. Claisse, D. A. Lopes, and P. Olsson, "Investigation of the ground- and metastable states of AnN (An = Th, Pu)," RSC Adv. **10**(42), 24877–24881 (2020).
[37]K. Kurosaki, K. Yano, K. Yamada, M. Uno, and S. Yamanaka, "A molecular dynamics study on plutonium mononitride," J. Alloys Compd. **313**(1–2), 242–247 (2000).

[38]M. Takano, M. Akabori, Y. Arai, and K. Minato, "Lattice thermal expansions of NpN, PuN and AmN," J. Nucl. Mater. **376**(1), 114–118 (2008).
[39]Y. Zhang, Z. Zhou, J. Lan, T. Bo, C. Ge, Z. Chai, and W. Shi, "Theoretical investigation on electronic and mechanical properties of ternary actinide (U, Np, Pu) nitrides," J. Appl. Phys. **122**(11), 115109 (2017).
[40]Z.-G. Mei, M. Stan, and B. Pichler, "First-principles study of structural, elastic, electronic, vibrational and thermodynamic properties of UN," J. Nucl. Mater. **440**(1–3), 63–69 (2013).
[41]S. C. Middleburgh, R. W. Grimes, K. H. Desai, P. R. Blair, L. Hallstadius, K. Backman, and P. Van Uffelen, "Swelling due to fission products and additives dissolved within the uranium dioxide lattice," J. Nucl. Mater. **427**(1–3), 359–363 (2012).
[42]V. Kocevski, D. A. Rehn, M. W. D. Cooper, and D. A. Andersson, "First-principles investigation of uranium mononitride (UN): Effect of magnetic ordering, spin-orbit interactions and exchange correlation functional," J. Nucl. Mater. **559**, 153401 (2022).
[43]S. I. Potashnikov, A. S. Boyarchenkov, K. A. Nekrasov, and A. Ya. Kupryazhkin, "High-precision molecular dynamics simulation of UO_2-PuO_2: Superionic transition in uranium dioxide," J. Nucl. Mater. **415**(2), 217–221 (2011).
[44]M. W. D. Cooper, S. T. Murphy, P. C. M. Fossati, M. J. D. Rushton, and R. W. Grimes, "Thermophysical and anion diffusion properties of $(U_x,Th_{1-x})O_2$," Proc. R. Soc. A **470**(2171), 20140427 (2014).
[45]M. W. D. Cooper, S. T. Murphy, M. J. D. Rushton, and R. W. Grimes, "Thermophysical properties and oxygen transport in the $(U_x,Pu_{1-x})O_2$ lattice," J. Nucl. Mater. **461**, 206–214 (2015).
[46]C. O. T. Galvin, M. W. D. Cooper, M. J. D. Rushton, and R. W. Grimes, "Thermophysical properties and oxygen transport in $(Th_x,Pu_{1-x})O_2$," Sci. Rep. **6**(10), 36024 (2016).
[47]J. Ma, J. Zheng, M. Wan, J. Du, J. Yang, and G. Jiang, "Molecular dynamical study of physical properties of $(U_{0.75}Pu_{0.25})O_{2-x}$," J. Nucl. Mater. **452**(1–3), 230–234 (2014).
[48]J. Ma, J. Du, M. Wan, and G. Jiang, "Molecular dynamics study on thermal properties of ThO_2 doped with U and Pu in high temperature range," J. Alloys Compd. **627**, 476–482 (2015).
[49]S. O. Vălu, O. Beneš, D. Manara, R. J. M. Konings, M. W. D. Cooper, R. W. Grimes, and C. Guéneau, "The high-temperature heat capacity of the $(Th,U)O_2$ and $(U,Pu)O_2$ solid solutions," J. Nucl. Mater. **484**, 1–6 (2017).
[50]X.-Y. Liu and D. A. Andersson, "Small uranium and oxygen interstitial clusters in UO_2: An empirical potential study," J. Nucl. Mater. **547**, 152783 (2021).
[51]B. Meredig, A. Thompson, H. A. Hansen, C. Wolverton, and A. van de Walle, "Method for locating low-energy solutions within DFT+U," Phys. Rev. B **82**(19), 195128 (2010).
[52]Y. Lu, B.-T. Wang, R.-W. Li, H. Shi, and P. Zhang, "Structural, electronic, and thermodynamic properties of UN: Systematic density functional calculations," J. Nucl. Mater. **406**(2), 218–222 (2010).
[53]K. O. Obodo and N. Chetty, GGA+U studies of the early actinide mononitrides and dinitrides," J. Nucl. Mater. **442**(1–3), 235–244 (2013).
[54]Y.-J. Zhang, J.-H. Lan, T. Bo, C.-Z. Wang, Z.-F. Chai, and W.-Q. Shi, "First-principles study of barium and zirconium stability in uranium mononitride nuclear fuels," J. Phys. Chem. C," **118**(26), 14579–14585 (2014).
[55]A. Claisse, M. Klipfel, N. Lindbom, M. Freyss, and P. Olsson, "GGA+U study of uranium mononitride: A comparison of the U-ramping and occupation matrix schemes and incorporation energies of fission products," J. Nucl. Mater. **478**, 119–124 (2016).
[56]C. Guéneau, A. Chartier, and L. Van Brutzel, *Thermodynamic and Thermophysical Properties of the Actinide Oxides* (Elsevier, 2012), Vol. 2.
[57]R. J. M. Konings, L. Morss, and J. Fuger, "Thermodynamic properties of actinides and actinide compounds," in *The Chemistry of the Actinide and Transactinide Elements*, edited by L. R. Morss, N. M. Fuger (Springer, Dordrecht., 2010).
[58]P. F. Weck, E. Kim, N. Balakrishnan, F. Poineau, C. B. Yeamans, and K. R. Czerwinski, "First-principles study of single-crystal uranium mono- and dinitride," Chem. Phys. Lett. **43**(1–3), 82–86 (2007).
[59]C. Affortit, "Chaleur specifique de UC et UN," J. Nucl. Mater. **34**(1), 105–107 (1970).
[60]J. B. Conway and P. N. Flagella, "Physical and mechanical properties of reactor materials GEMP-1012," Technical report (General Electric Company, 1969).
[61]T. R. Pavlov, M. R. Wenman, L. Vlahovic, D. Robba, R. J. M. Konings, P. Van Uffelen, and R. W. Grimes, "Measurement and interpretation of the thermophysical properties of UO_2 at high temperatures: The viral effect of oxygen defects," Acta Mater. **139**, 138–154 (2017).
[62]V. G. Baranov, A. V. Lunev, V. V. Mikhalchik, A. V. Tenishev, and D. P. Shornikov, "High temperature behavior of simulated mixed nitrides," IOP Conf. Ser.: Mater. Sci. Eng. **130**(1), 012022 (2016).
[63]F. L. Oetting, "The chemical thermodynamic properties of nuclear materials. III. Plutonium mononitride," J. Chem. Thermodyn. **10**(10), 941–948 (1978).
[64]C. A. Alexander, R. B. Clark, O. L. Kruger, and J. L. Robins, "Fabrication and high temperature thermodynamic and transport properties of PuN." in *Plutonium 1975 and other actinides: proceedings of the Conference in Baden Baden*, September 10–13, 1975/5th International Conference on Plutonium and Other Actinides, 1975, edited by H. Blank and R. Lindner (North-Holland Publishing Company, 1975).
[65]K. E. Spear and J. M. Leitnaker, "A consistent set of thermodynamic values for plutonium mononitride," J. Am. Ceram. Soc. **51**(12), 706–709 (1968).